Atmos. Chem. Phys. Discuss., 12, 32707–32739, 2012
www.atmos-chem-phys-discuss.net/12/32707/2012/
doi:10.5194/acpd-12-32707-2012

Atmospheric Chemistry and Physics Discussions

Mixing state of individual submicron carbon-containing particles and their seasonal variation in urban Guangzhou, China

G. Zhang[1,2], X. Bi[1], L. Li[3], L. Y. Chan[1], M. Li[3], X. Wang[1], G. Sheng[1], J. Fu[1,3], and Z. Zhou[3]

[1]State Key Laboratory of Organic Geochemistry, Guangzhou Institute of Geochemistry, Chinese Academy of Sciences, Guangzhou 510640, China
[2]Graduate University of Chinese Academy of Sciences, Beijing 100039, China
[3]School of Environmental and Chemical Engineering, Shanghai University, Shanghai 200444, China

Received: 30 October 2012 – Accepted: 22 November 2012 – Published: 19 December 2012

Correspondence to: X. Bi (bixh@gig.ac.cn)

Published by Copernicus Publications on behalf of the European Geosciences Union.

Abstract

Growing evidence suggests that size-resolved mixing state of carbon-containing particles is very critical in determining their optical properties, atmospheric lifetime, and impact on the environment. However, still little is known about the mixing state of particles in urban area of Pearl River Delta (PRD) region, China. To investigate the mixing state of submicron carbon-containing particles, measurements were carried out during spring and fall periods of 2010 using a single particle aerosol mass spectrometer (SPAMS). Approximate 700 000 particles for each period were detected. This is the first report on the size-resolved mixing state of carbon-containing particles by direct observations in PRD region. Cluster analysis of single particle mass spectra was applied to identify carbon-containing particle classes. These classes represented ~ 80 % and ~ 90 % of all the detected particles for spring and fall periods, respectively. Carbon-containing particle classes mainly consisted of biomass/biofuel burning particles (Biomass), organic carbon (OC), fresh elemental carbon (EC-fresh), internally mixed OC and EC (ECOC), internally mixed EC with sulfate (EC-Sulfate), vanadium-containing ECOC (V-ECOC), and amines-containing particles (Amine). In spring, the top three ranked carbon-containing particle classes were ECOC (26.1 %), Biomass (23.6 %) and OC (10 %), respectively. However, the fraction of Biomass particles increased remarkably and predominated (61.0 %), while the fraction of ECOC (3.0 %) and V-ECOC (0.1 %) significantly decreased in fall. To highlight the influence of monsoon on the properties of carbon-containing particles in urban Guangzhou, their size distribution, mixing state, and aerosol acidity were compared between spring and fall seasons. In addition, a case study was also performed to investigate how the formation of fog and haze influenced the mixing state of carbon-containing particles. These results are of importance in understanding atmospheric chemistry and modeling direct and indirect forcing of carbon-containing particles.

ACPD

12, 32707–32739, 2012

1 Introduction

Carbonaceous aerosols represent a major fraction of submicron aerosol particles in urban and heavily industrialized areas in China (Chan and Yao, 2008). They strongly affect the visibility and energy balance of the Earth by either scattering or absorbing solar radiation (Jacobson, 2001; Ramanathan and Carmichael, 2008). They contribute to an indirect effect on global climate acting as cloud condensation nuclei (CCN) (Sun and Ariya, 2006; Jacobson, 2006). Depending on particle size and chemical composition, they may also cause severe health problems (Pöschl, 2005; Turpin and Huntzicker, 1995). Therefore, carbonaceous aerosols have been the focus of atmospheric aerosol researches for several decades.

Carbonaceous aerosols are normally divided into two major fractions: organic carbon (OC) and elemental carbon (EC). OC could be directly emitted into the atmosphere from both anthropogenic and natural sources, and also formed via conversion of volatile precursors (Chung and Seinfeld, 2002; Jacobson et al., 2000). Numerous ambient measurements have found that organic matters represented a significant and highly variable fraction of atmospheric aerosols, typically varying between 20 % and 90 % of fine particulate mass (Kanakidou et al., 2005). EC is generated exclusively by incomplete combustion processes such as vehicular exhaust (Huang et al., 2006), biomass burning (Andreae, 1983), and coal combustion (Chen et al., 2006), and it mainly exists in submicron sizes and represents relatively low fraction compared to OC (Clarke et al., 2004; Yu et al., 2010).

Generally, OC is believed to primarily scatter visible light, while some organic components could absorb solar radiation (Andreae and Gelencser, 2006; Kirchstetter et al., 2004). Recent studies have also suggested that OC represents an important part of the global CCN budget (Riipinen et al., 2011), and its activation capability might be comparable to that of sulfate aerosols (Sun and Ariya, 2006). Furthermore, OC could alter the hygroscopic properties and CCN activity of inorganic species as a function of its mixing states (Svenningsson et al., 2006). EC is a primary light absorption con-

ACPD
12, 32707–32739, 2012

stituent in the atmosphere and it significantly contributes to positive radiative forcing (Jacobson, 2001). The optical properties of EC are strongly dependent on its mixing state. Previous studies reported that presence of coating materials such as OC and sulfate on EC surface could substantially enhance absorption ability of EC (Moffet and Prather, 2009). Atmospheric heterogeneous chemistry on EC surface could also be affected when it internally mixed with other species (Adachi and Buseck, 2008; Johnson et al., 2005). Therefore, it is of substantial importance to figure out the mixing state of carbon-containing particles, in order to improve our understanding on their atmospheric process.

Situated in the Pearl River Delta (PRD) region, the atmospheric condition of Guangzhou is under a strong influence of the Asian monsoon system. Southwesterly to southeasterly monsoon brings relatively clean air from the sea in summer and spring, and northeasterly wind carries relatively polluted air masses across northern cities in fall and winter. The inherent seasonality in monsoon circulation results in dryness during fall and winter, and wetness during spring and summer. Measurements showed that the attenuation of light caused by carbonaceous aerosols was potentially important in the PRD region (Cheng et al., 2008; Yu et al., 2010). The number fraction of internally mixed EC was highly variable and can be as high as ~70 % (Huang et al., 2012). Knowledge on mixing state of carbon-containing particles is a necessary prerequisite to accurately determine their contribution to the visibility degradation and to understand their roles in the regional climate. However, direct observations on the size-resolved mixing state of carbon-containing in the PRD region or in the other parts of China were scarce (e.g. Fu et al., 2012; Li et al., 2010; Huang et al., 2012).

An experiment was carried out in urban Guangzhou during spring and fall periods, using a single particle aerosol mass spectrometer (SPAMS). The aim is (1) to reveal the major single particle classes of carbon-containing particles, and (2) to picture the influence of Asian monsoon on their number fraction as a function of aerodynamic diameter (d_{va}), mixing state with secondary species, and particle acidity in the urban area of PRD region, China.

ACPD
12, 32707–32739, 2012

2 Experiment set-up and data analysis

2.1 Meteorological conditions during the sampling

Single particle measurements were carried out at Guangzhou Institute of Geochemistry (GIG), Chinese Academy of Sciences, during late spring (between 30 April and 22 May of 2010), and fall (between 5–20 November of 2010), using a SPAMS (Li et al., 2011) developed by Hexin Analytical Instrument Co., Ltd. (Guangzhou, China). Measurement site was described elsewhere (Bi et al., 2011). The ambient temperature during sampling in spring varied between 19–33 °C, with an average of 26 °C; and average relative humidity (RH) was 81 % with ranging between 22–100 %. The ambient temperature during fall period was in the range of 16–38 °C, with an average of 23 °C; and average RH was 54 % with 21 % lowest and 82 % highest. Twenty four hour air mass back-trajectory for each day (ending at 00:00 LT) during both spring and fall was calculated by HYSPLIT 4.9 transport model (http://ready.arl.noaa.gov/HYSPLIT.php) (Draxler and Rolph, 2012). Based on the model, air masses from southeastern and southwestern marine region dominated throughout the spring, while during the fall air masses from northeastern continental areas were prevalent (see Fig. S1 in Supplement).

2.2 Methodology of single particle detection and data analysis

The particle detection method of SPAMS was described by Li et al. (2011). Briefly, aerosol particles are introduced into SPAMS through a critical orifice, then focused and accelerated to specific velocities, which are determined by their flight time through two continuous diode Nd : YAG laser beams (532 nm) in sizing region. The particles are subsequently desorped/ionized by a pulsed laser (266 nm) triggered exactly based on the velocity of the specific particle. The positive and negative fragments generated are recorded with its d_{va}.

In this study, approximate 700 000 particles for each period, with d_{va} ranging between 0.2 and 1.2 µm, were chemically analyzed with both positive and negative ion spectra.

ACPD
12, 32707–32739, 2012

Particle size and mass spectra information were used to create the peak lists with a minimum area threshold of 20 arbitrary units (background noise was generally lower than 5 units) by using TSI MS-Analyze software. The peak lists were then imported into MATLAB (The Mathworks Inc.) and analyzed with YAADA 2.1 (http://www.yaada.org). Peak identification described in this paper corresponded to the most probable assignments for each particular mass to charge ratio (m/z). An adaptive resonance theory based neural network algorithm (ART-2a) was applied to cluster individual particles into separate groups based on the presence and intensity of ion peaks in individual single particle mass spectra (Song et al., 1999) with a vigilance factor of 0.75, learning rate of 0.05, and 20 iterations. First 250 clusters in spring and 200 clusters in fall dominated the initially generated clusters, representing more than 90 % of all the analyzed particles, and were manually merged to produce 11 and 10 final particle classes based on the spectral similarities, respectively.

2.3 Scanning mobility particle sizer with a condensation particle counter (SMPS + C)

Particle size distribution measurements were performed using a cylindrical scanning differential mobility analyzer upstream of a condensation particle counter (SMPS + C 5.401, GRIMM Aerosol Technik GmbH & Co. KG) during 7–21 May 2010 (Zhang et al., 2012). Size distribution reading from SMPS + C referred in the discussion section of this paper only included the particles with d_m lower than 521 nm. Particle number concentration obtained from the collocated SMPS + C was commonly utilized to scale the particle number counts from SPAMS, in order to obtain an approximately quantitative view (e.g. Reinard et al., 2007; Bein et al., 2006; Healy et al., 2012), although it might introduce an error in scaled number counts for different particle classes (Gross et al., 2006). The size-dependent hourly scaling factors are shown in Fig. S2. It is noted that the collocated SMPS + C was only operated for approximate 174 h while SPAMS ran 376 h during the spring sampling period. Thus the quantitative results mentioned after this point only are referred to the period when the collocated SMPS + C was operated.

ACPD
12, 32707–32739, 2012

3 Results and discussion

The chemical components of the analyzed particles were determined through classifying particles into the distinct catalogues. As listed in Table 1, seven out of eleven and six out of ten single particle classes during spring and fall periods were assigned as carbon-containing particles, referring to particle classes containing OC, EC, or their combinations (Liu et al., 2003; Bahadur et al., 2010). Carbon-containing particles consisted of particle classes corresponding to biomass/biofuel burning particles (Biomass), OC-dominant particles lacking or with negligible EC signals (OC), internally mixed OC and EC (ECOC), fresh EC particles (EC-fresh), EC-dominant particles mainly mixed with sulfate (EC-Sulfate), and vanadium-containing ECOC (V-ECOC). In addition, there was an amines-containing particle class (Amine), and it was unique to spring period. Carbon-containing particle classes described here resembled those observed in Mexico city by Moffet et al. (2008). Other single particle classes, such as dust and sea salt, were grouped together with unclassified particles as "Others".

Overall, the average digitized mass spectrum (Fig. 1) of carbon-containing particles shows that 39 $[K]^+$, dual polarity EC cluster ions (12 $[C]^{+/-}$, 24 $[C_2]^{+/-}$, 36 $[C_3]^{+/-}$, ..., $[C_n]^{+/-}$), as well as fragments from secondary inorganic species sulfate ($-97[HSO_4]^-$), nitrate ($-46[NO_2]^-$ and $-62[NO_3]^-$), and ammonium ($18[NH_4]^+$) were the dominant peaks. However, the peak at m/z 39 may also be assigned to an organic fragment $39[C_3H_3]^+$ (Silva and Prather, 2000) when organics dominate in particles. Most of carbon-containing particles internally mixed with sulfate and/or nitrate, indicating some degree of atmospheric ageing (Toner et al., 2008). Other dominant peaks at m/z $15[CH_3]^+$, $27[C_2H_3]^+$, $29[C_2H_5]^+$, $37[C_3H]^+$, $43[C_2H_3O]^+$, $51[C_4H_3]^+$, $55[C_4H_7]^+$, $57[C_4H_9]^+$ and $63[C_5H_3]^+$ were typically characteristic of signals due to the organic fragments (Silva and Prather, 2000), while lower fraction of the organic fragments at m/z $77[C_6H_5]^+$ and $91[C_7H_7]^+$ were also observed in the mass spectra. The peak series at m/z 51, 63, 77 and 91 are indicative of aromatic signature (Dall'Osto and Harrison, 2012; Silva and Prather, 2000). In addition, peaks corresponding to sodium

ACPD
12, 32707–32739, 2012

(23[Na]$^+$), calcium (40[Ca]$^+$), and vanadium (51[V]$^+$/67[VO]$^+$) in the positive mass spectra, and −26[CN]$^-$ and −42[CNO]$^-$ in the negative mass spectra were also detected. The complex mixture of these particles could be attributed to different sources and/or the extensive processing of carbon-containing particles in the atmosphere.

3.1 Single particle classes of carbon-containing particles

Average positive and negative mass spectra for the carbon-containing particle classes for the spring period are presented in Fig. 2, while the results for the fall were similar and presented in Fig. S3. A brief description of mass spectral characteristic of these particle classes was provided as follow:

The mass spectra of Biomass particles presented potassium (39[K]$^+$) as the highest peaks, combined with carbonaceous ion peaks, and also K cluster ions with Cl^- (113[$K_2{}^{35}Cl$]$^+$/115[$K_2{}^{37}Cl$]$^+$) and with SO_4^{2-} (213[$K_3{}^{32}SO_4$]$^+$/215[$K_3{}^{34}SO_4$]$^+$) in relatively low intensity, indicating the biomass origin nature of these particles (Liu et al., 2003; Pratt et al., 2011). The negative ion markers, at m/z −45, −59, and −73 due to levoglucosan, for biomass burning particles was also detected in these particles although they were in low intensity (Bi et al., 2011). Additionally, peaks corresponding to sulfate and nitrate were commonly observed in the negative mass spectrum, which means that Biomass particles were subjected to atmospheric ageing and acquired a large amount of sulfate and nitrate during transport (Pratt et al., 2011).

ECOC particles were characterized by positive mass spectrum that were dominated by EC cluster ions, intense OC signals (e.g. m/z 27, 37, 39 and 43), nitrate, sulfate, and ammonium. Median peaks at 51[C_4H_3]$^+$, 63[C_5H_3]$^+$ attributed to aromatic compounds were also observed. There was another ECOC particle type: V-ECOC, which provides a very unique mass spectrum due to strong ion peaks from 51[V]$^+$/67[VO]$^+$. Vanadium-containing particles have been detected in the ambient aerosols (Tolocka et al., 2004; Moffet et al., 2008), and are attributed to residual fuel oil combustion associated with sources such as ships and refineries (Moldanová et al., 2009; Ault et al., 2010), and to vehicle exhausts of minor fraction (Sodeman et al., 2005; Shields et al., 2007).

ACPD
12, 32707–32739, 2012

EC-fresh particles were dominated by dual polarity EC cluster ions with really low intensity of secondary species. It is noted that EC-fresh particles were actually not pure EC but dominated by EC composition since EC-fresh particles usually consisted of weak ion peaks from OC and sulfate. The strongest signals for 23$[Na]^+$ and 40$[Ca]^+$ were observed in this particle type. Ca-containing EC particles has previously been detected in the combusted lubricating oil emitted by automobiles (Dall'Osto et al., 2009; Spencer et al., 2006), despite the fact that the strong intensity of K may still indicate the biomass/biofuel origin of this particle type. Therefore, this particle type represented a mixture of fresh EC particles from these two combustion processes. Similar to the EC-fresh, EC-Sulfate particles comprised of peaks from strong EC cluster ions with strong sulfate signature, but weak signals from nitrate. While m/z −97 might also be assigned to phosphate $[H_2PO_4]^-$ for particles from fresh vehicle exhaust (Toner et al., 2006), the absence of coexistence fragment at m/z −79$[PO_3]^-$ suggests the correct assignment of m/z −97 to $[HSO_4]^-$. These particles were also observed in the urbanized Mexico City and it suggested that they were produced by an oxidation of sulfur in the fuel and rapid condensation onto the existing EC particles in the plume (Moffet and Prather, 2009).

There were two classes of OC dominant particles: OC and Amine. Unlike ECOC particles, mass spectra of OC particles were dominated by intense OC signals (e.g. m/z 27, 37, 39 and 43). Intense peak corresponding to sulfate was also observed in these particles. Amine particles showed distinct ion peak at m/z +59 ($[N(CH_3)_3]^+$), which was assigned to trimethylamine (Angelino et al., 2001; Rehbein et al., 2011). This particle type was exclusively observed during the spring period and significantly enhanced through the fog processing as previously reported by our group and the others (Rehbein et al., 2011; Zhang et al., 2012). The relatively dry air condition (RH: 54 %) during fall period was probably responsible for the missing of Amine class, since the aerosol water evidentially seemed to be the dominant factor to control the gas-to-particle conversion of trimethylamine (Rehbein et al., 2011).

ACPD
12, 32707–32739, 2012

3.2 Seasonal variations of carbon-containing particles

Table 1 lists number fraction of carbon-containing classes calculated based on the unscaled particle number count, with the scaled result during spring period. Although the unscaled number fractions only provided the indicative results, and they could not represent the quantitative information, the differences still can be seen between spring and fall seasons. During spring period, the top three carbon-containing particle classes were ECOC (26.1 %), Biomass (23.6 %) and OC (10 %), respectively. EC-Sulfate (8.6 %) showed a moderate contribution, while the last three classes were EC-fresh (4.6 %), Amine (3.4 %) and V-ECOC (1.9 %). During fall period, the fraction of Biomass particles increased considerably and predominated (61.0 %), however, the fraction of V-ECOC (0.1 %) and ECOC (3.0 %) significantly decreased and Amine particles were absent during this period.

Considerable increase of Biomass particles during the fall period suggests the significant influence of regional biomass burning activities on the ambient air quality of urban Guangzhou during the fall period. A fire dot maps (Fig. S4), obtained from the Moderate Resolution Imaging Spectroradiometer (MODIS) on board the Terra and Aqua satellites over a 10-day period, showed that fire dots in the Northeast of Guangzhou were intense during fall period, and the air parcels from these areas brought in large amount of biomass burning particles. Zhang et al. (2010) also suggested a similar impact of biomass burning activities in neighboring and/or rural regions on ambient urban aerosol level in PRD region. Although during spring period there were also many fire dots in the neighboring regions (Fig. S4), the dominant air masses from oceanic areas and the relatively abundance of precipitation resulted in minimizing the influence of biomass burning on the air quality. With dissimilarity to Biomass particles, V-ECOC particles were rarely detected during the fall period (0.1 %) compared to those during the spring period (1.9 %), which can be interpreted by the fact that the air masses originated from marine areas were prevalent during the spring period and ship emission was suspected to be a dominant source for V-ECOC. A higher fraction of V-ECOC in

ACPD
12, 32707–32739, 2012

larger particles (Fig. 3) probably supported this air mass history and its long range transport. Considering more stagnant meteorological condition during the fall should facilitate the formation of SOA on particle cores like EC, the significant decrease in number fraction of ECOC was unexpected and the reason behind this was unclear. With regard to a discussion in the next section, the difference was likely to attribute to the size distribution of EC-Sulfate between spring and fall seasons.

3.2.1 Chemically-resolved size distribution

Figure 3 shows the size-resolved number fraction of single particle classes, which was highly variable with d_{va}. For example, during spring period, EC-fresh and EC-Sulfate particles dominated in the size range of 0.2–0.3 µm, together accounting for 72 % in this size range, while they were less than 13 % in the size range of 0.4–1.2 µm. The most abundant of EC-Sulfate in the smaller particles might indicate a predominant role of sulfuric acid in the processing EC (Khalizov et al., 2009). Dominant number fraction of EC was found from the fresh vehicle exhausts in the submicron range (Shields et al., 2007) and ultrafine size ranges (< 0.2 µm) (Sodeman et al., 2005). OC and ECOC classes were the minor fraction (less than 3 %) in the size range of 0.2–0.3 µm, implying that EC and OC were more externally mixed in the smaller particles.

Chemical pattern during spring period changed substantially from the smaller (0.2–0.4 µm) to the larger particles (0.4–1.2 µm) (Fig. 3a). The number fractions of EC-fresh and EC-Sulfate presented a similar pattern as a function of d_{va}. They decreased dramatically, while the OC and ECOC classes increased considerably from the smaller to the larger particles. Increased ECOC in the larger particles might be caused by ageing of EC-fresh and EC-Sulfate in the smaller particles through the condensation of semi-volatile species (e.g. ammonium, nitrate and organics) and/or hygroscopic growth, when considering the internal mixing with sulfuric acid dominating the initial ageing processes (Khalizov et al., 2009). Once emitted into the air, the irregular geometry and complex microstructure of EC may provide the active sites for following ageing (Decesari et al., 2002).

ACPD
12, 32707–32739, 2012

The major difference of size fraction distributions between spring and fall periods were the Biomass particles (Fig. 3). It is observed that relative intensity of the secondary species (i.e. ammonium (m/z 18), organics (m/z 43), nitrate (m/z −62) and sulfate (m/z −97)) increased from the smaller to the larger Biomass particles, during both periods. The increase of these species was much stronger during the fall period than the spring period, particularly the nitrate and sulfate (Fig. S5). This might indicate the emission of the Biomass particles more likely to be the local and regional sources during spring period, while larger contribution of long range transport was expected to occur in the fall period. Additionally, the number fraction of EC-Sulfate generally increased from 0.3–1.2 µm with d_{va} during the fall period (Fig. 3b), which did not happen during the spring period. In the fall, these particles contained much greater intense K^+ peak than the spring, and their temporal trend also highly correlated to the Biomass particles ($r = 0.75$, $p < 0.001$). The results indicate considerable contribution of the biomass burning to EC-Sulfate particles from long range transport, which would lead to larger EC-Sulfate particles during fall period.

The different size distribution pattern of EC-Sulfate particles may contribute to the difference between number fractions of ECOC during the spring and fall periods. It is obvious that the number fraction of EC-Sulfate particles in the size range of 0.2–0.4 µm was higher in the spring than the fall. Generally, the smaller particle number concentration was much higher than the larger particles. Thus a large number of EC-Sulfate particles in the smaller particles would provide sufficient EC core for the ECOC formation, which might lead to increase in number fraction of ECOC type in the spring.

3.2.2 Mixing state

The mixing state of carbon-containing particle classes with the secondary species was also explored. The presence of secondary species on the various carbon-containing particle classes provides an indication of chemical processes. Markers (i.e. m/z 18, −62 and −97) were selected to represent the secondary inorganic species. The organic carbon marker, m/z 43, is selected as a secondary organic species, which could be

ACPD
12, 32707–32739, 2012

formed by oxidation reactions and gas-to-particle conversion of organic species (Moffet and Prather, 2009).

Figure 4 displays the mixing state of secondary markers on the various carbon-containing particle classes. The larger amount of ammonium was observed during the fall period, and was attributed to the northeastern air masses from agricultural areas. The enhanced fractions of sulfate and oxidized organics were also found in the carbon-containing particle. More radiation during the fall period might be favorable for the production of sulfate and oxidized organics through the photo-chemical reactions (Xiao et al., 2009), which was uncommon during the rainy spring period. However, the number fraction of nitrate on the carbon-containing particle classes decreased during the spring through the fall. The decrease of nitrate was probably due to the relatively dry air (Hu et al., 2008), and the reduction of its gaseous precursors mainly emitted from the local traffic and industry (Wang et al., 2008), as a result of an air quality guarantee program during the Asian Games in Guangzhou between 1 November and 20 December 2010, when half of the motor vehicles were off the road and many industrial facilities were shut down.

It is interesting to note that nitrate preferred to associate with the Biomass and OC particles during the fall period, and about 44 % and 62 % of the Biomass and OC particles had nitrate signals, while the fractions varied between 10–33 % in the other particles. Meanwhile nitrate showed larger peak areas in the Biomass and OC particles (Fig. S3). The dependency of nitrate formation on the particles chemical compositions during the fall period might suggest a heterogeneous reaction of HNO_3 or NO_2 on the mineral-rich particles like the Biomass particles. The strong association of nitrate with OC might indicate the present of organic nitrate probably formed from the NO_3 radical-initiated oxidation of volatile organic compounds (Zaveri et al., 2010). However, nitrate distributed more evenly during the spring period. This is due to the different formation mechanism. Hydrolysis of NO_3 and N_2O_5 is potentially to be the major pathway of particulate nitrate under high RH (Pathak et al., 2011), thus it would distribute the nitrate

ACPD
12, 32707–32739, 2012

more evenly among particle types of a similar size and would not strongly depend on the chemistry of the original particle type.

3.2.3 Variation of particle acidity

Here we adopted the relative acidity ratio (R_{ra}) calculated by Denkenberger et al. (2007). The R_{ra} was defined as a sum of absolute average peak areas of nitrate (m/z −62) and sulfate (m/z −97) divided by that of ammonium (m/z 18), to represent the aerosol acidity. Although it does not provide the quantitative information on the particle acidity, it might be indicative. The dependence of R_{ra} on d_{va} is presented in Fig. 5 for the spring and fall periods, respectively. In general, R_{ra} decreased from the smaller to the larger particles for the carbon-containing particle classes. R_{ra} for carbon-containing particle classes were larger during the spring than the fall period, consistent with the higher fraction of ammonium causing low acidity of the particles in the fall. Although low intensity, more than 50 % of EC-fresh particles were found to contain the sulfate signals. The higher relative acidity ratio of EC-fresh in the smaller particles suggested a rapid condensation of sulfuric acid onto the EC surface.

During the spring period, R_{ra} values for the EC-Sulfate particles were obviously larger than those for other particle classes, especially in the size range of 0.2–0.4 µm. It is worthy to note that the EC-Sulfate particles contained low fraction of ammonium (35 %) and nitrate (35 %), compared to sulfate (97 %), as shown in Fig. 4. This implies that a certain fraction of sulfate might exist in the form of sulfuric acid rather than ammonium bisulfate and/or ammonium sulfate salts, despite of low efficiency of ammonium due to a laser ionization (Gross et al., 2000). The lowest relative acidity ratio for Amine particles was expected since these particles contained a large amount of ammonium (Zhang et al., 2012).

ACPD
12, 32707–32739, 2012

3.3 Case study of carbon-containing particles under specific meteorological conditions

Carbon-containing particles during typical periods in the spring and fall were further investigated to highlight the influence of meteorological conditions. Figure 6 shows the hourly scaled number concentration of single particle classes in the size range of 0.2–0.95 µm during 19–22 May 2010 of the spring period, when typical weather conditions (i.e. rain, fog and cloudy, as marked in the figure) were observed. Rain generally reduced the particle number concentration through the wet deposition. A significant scavenge of particles was obtained during a heavy rain as marked in the midday on 21 May, with the number concentration decreasing from $\sim 1.7 \times 10^4$ to $\sim 0.5 \times 10^4$ cm^{-3}. The foggy episode was identified with the ambient relative humidity exceeding 90 % and the fog processing marker hydroxymethanesulfonate (Munger et al., 1986; Whiteaker and Prather, 2003), and the details could be found elsewhere (Zhang et al., 2012). During foggy episode, the particle number concentration increased predominantly as a result of the relatively stagnant meteorological condition, and also probably the contribution from the growth of smaller particles to fit with the detectable size range of SPAMS.

The fog processing is expected to influence the chemistry of aerosols. The difference between mass spectra of carbon-containing particles before and after the foggy episode is illustrated in Fig. 7. Through the fog processing, OC, ECOC, V-ECOC and EC-Sulfate were generally enhanced with the secondary inorganic species (sulfate, nitrate and/or ammonium). The enhanced secondary inorganic species in aerosols were commonly observed throughout the foggy episodes (Biswas et al., 2008; Safai et al., 2008). However, the EC-fresh and Biomass particles were probably freshly emitted more during the episode, so there was no obvious variation of the secondary species in their mass spectra.

During the fall period, two severe hazy episodes were identified on the 5–6 and 15–17 November 2010, with atmospheric visibility as low as 1.7 and 4 km for Haze 1 and Haze 2, respectively. Unlike the foggy episode, the number fraction of carbon-

ACPD
12, 32707–32739, 2012

containing particle classes only showed slightly variation from the cloudy to hazy days. However, the relative intensity of secondary species generally showed an increase from the cloudy to the hazy days (see Fig. 8). The results in this study is consistent with our previous off-line filter measurements conducted in urban Guangzhou (Tan et al., 2009), in which the secondary species were found considerably enhanced on the hazy days.

4 Conclusions

In this study, we provide the direct observation of size-resolved mixing state characteristic of carbon-containing particles in urban Guangzhou during the spring and fall periods, 2010. The carbon-containing particles dominated the particles in submicron size range (0.2–1.2 µm) in the present study, and were general characteristic of the distinct single particle classes (Biomass, OC, ECOC, EC-fresh, EC-Sulfate, V-ECOC and Amine). The spring-fall contrast in prevailing air mass transport might be associated with the seasonal variations of chemical pattern, size distribution, mixing state, and aerosol acidity of carbon-containing particles in the urban area of PRD region.

During the spring period, air masses dominated from the marine region impacted ambient atmosphere in urban Guangzhou, with many more V-ECOC and sea salt particles. During the fall period, the persistent northeast monsoon during the fall period brought pollutants emitted from the potential source regions in the Southeastern China, and this resulted in significant contribution from the Biomass particles. The relative number fractions of carbon-containing particle classes were strongly variable with d_{va}. The high amount of pure EC particles (i.e. externally mixed) and extensively mixed EC and sulfate were obtained in the size range of 0.2–0.4 µm, particularly during the spring period. The mixing state and particle acidity of carbon-containing particle classes also varied substantially from the spring to fall periods. Air masses from the northeastern agricultural areas imported a large amount of ammonia into the urban Guangzhou, therefore it contributed to the low acidity of aerosols during the fall period. Case study under the specific meteorological condition also showed that foggy and hazy episodes

ACPD
12, 32707–32739, 2012

might also take part in the processing of carbon-containing particles, through the combination of number fraction and peak area analysis on the carbon-containing particle classes association with the secondary species. These results, by direct single particle observation, could improve our understanding on the atmospheric chemistry and also help to reduce the uncertainty of modeling their climate forcing relating to the carbon-containing particles.

Supplementary material related to this article is available online at: http://www.atmos-chem-phys-discuss.net/12/32707/2012/acpd-12-32707-2012-supplement.pdf.

Acknowledgement. This work was supported by the National Nature Science Foundation of China (No. 41073077), Guangzhou Institute of Geochemistry (GIGCAS 135 project Y234161001), and State Key Laboratory of Organic Geochemistry (SKLOG2011A01). We thank Zhengxu Huang for his assistance during sampling and instrument maintenance. The authors also gratefully acknowledge the NOAA Air Resources Laboratory (ARL) for the provision of the HYSPLIT transport and dispersion model and/or READY website (http://ready.arl.noaa.gov) used in this publication. This is contribution no. 1589 from GIGCAS.

References

Adachi, K. and Buseck, P. R.: Internally mixed soot, sulfates, and organic matter in aerosol particles from Mexico City, Atmos. Chem. Phys., 8, 6469–6481, doi:10.5194/acp-8-6469-2008, 2008.

Andreae, M. O.: Soot carbon and excess fine potassium – long-range transport of combustion-derived aerosols, Science, 220, 1148–1151, 1983.

Andreae, M. O. and Gelencsér, A.: Black carbon or brown carbon? The nature of light-absorbing carbonaceous aerosols, Atmos. Chem. Phys., 6, 3131–3148, doi:10.5194/acp-6-3131-2006, 2006.

ACPD

12, 32707–32739, 2012

Angelino, S., Suess, D. T., and Prather, K. A.: Formation of aerosol particles from reactions of secondary and tertiary alkylamines: characterization by aerosol time-of-flight mass spectrometry, Environ. Sci. Technol., 35, 3130–3138, 2001.

Ault, A. P., Gaston, C. J., Wang, Y., Dominguez, G., Thiemens, M. H., and Prather, K. A.: Characterization of the single particle mixing state of individual ship plume events measured at the port of Los Angeles, Environ. Sci. Technol., 44, 1954–1961, doi:10.1021/es902985h, 2010.

Bahadur, R., Russell, L., and Prather, K.: Composition and morphology of individual combustion, biomass burning, and secondary organic particle types obtained using urban and coastal ATOFMS and STXM-NEXAFS measurements, Aerosol Sci. Tech., 44, 551–562, doi:10.1080/02786821003786048, 2010.

Bein, K. J., Zhao, Y., Pekney, N. J., Davidson, C. I., Johnston, M. V., and Wexler, A. S.: Identification of sources of atmospheric PM at the Pittsburgh supersite – Part II: Quantitative comparisons of single particle, particle number, and particle mass measurements, Atmos. Environ., 40, 424–444, doi:10.1016/j.atmosenv.2006.01.064, 2006.

Bi, X. H., Zhang, G. H., Li, L., Wang, X. M., Li, M., Sheng, G. Y., Fu, J. M., and Zhou, Z.: Mixing state of biomass burning particles by single particle aerosol mass spectrometer in the urban area of PRD, China, Atmos. Environ., 45, 3447–3453, doi:10.1016/j.atmosenv.2011.03.034, 2011.

Biswas, K. F., Ghauri, B. M., and Husain, L.: Gaseous and aerosol pollutants during fog and clear episodes in South Asian urban atmosphere, Atmos. Environ., 42, 7775–7785, doi:10.1016/j.atmosenv.2008.04.056, 2008.

Chan, C. K. and Yao, X.: Air pollution in mega cities in China, Atmos. Environ., 42, 1–42, doi:10.1016/j.atmosenv.2007.09.003, 2008.

Chen, Y. J., Zhi, G. R., Feng, Y. L., Fu, J. M., Feng, J. L., Sheng, G. Y., and Simoneit, B. R. T.: Measurements of emission factors for primary carbonaceous particles from residential raw-coal combustion in China, Geophys. Res. Lett., 33, L20815, doi:10.1029/2006gl026966, 2006.

Cheng, Y. F., Wiedensohler, A., Eichler, H., Su, H., Gnauk, T., Brüggemann, E., Herrmann, H., Heintzenberg, J., Slanina, J., Tuch, T., Hu, M., and Zhang, Y. H.: Aerosol optical properties and related chemical apportionment at Xinken in Pearl River Delta of China, Atmos. Environ., 42, 6351–6372, 2008.

ACPD

12, 32707–32739, 2012

Chung, S. and Seinfeld, J.: Global distribution and climate forcing of carbonaceous aerosols, J. Geophys. Res., 107, 4407, doi:10.1029/2001JD001397, 2002.
Clarke, A. D., Shinozuka, Y., Kapustin, V. N., Howell, S., Huebert, B., Doherty, S., Anderson, T., Covert, D., Anderson, J., Hua, X., Moore, K. G., McNaughton, C., Carmichael, G., and Weber, R.: Size distributions and mixtures of dust and black carbon aerosol in Asian outflow: physiochemistry and optical properties, J. Geophys. Res.-Atmos., 109, D15S09, doi:10.1029/2003JD004378, 2004.
Dall'Osto, M. and Harrison, R. M.: Urban organic aerosols measured by single particle mass spectrometry in the megacity of London, Atmos. Chem. Phys., 12, 4127–4142, doi:10.5194/acp-12-4127-2012, 2012.
Dall'Osto, M., Harrison, R. M., Coe, H., and Williams, P.: Real-time secondary aerosol formation during a fog event in London, Atmos. Chem. Phys., 9, 2459–2469, doi:10.5194/acp-9-2459-2009, 2009.
Decesari, S., Facchini, M. C., Matta, E., Mircea, M., Fuzzi, S., Chughtai, A. R., and Smith, D. M.: Water soluble organic compounds formed by oxidation of soot, Atmos. Environ., 36, 1827–1832, doi:10.1016/s1352-2310(02)00141-3, 2002.
Denkenberger, K. A., Moffet, R. C., Holecek, J. C., Rebotier, T. P., and Prather, K. A.: Real-time, single-particle measurements of oligomers in aged ambient aerosol particles, Environ. Sci. Technol., 41, 5439–5446, doi:10.1021/es070329l, 2007.
Fu, H., Zhang, M., Li, W., Chen, J., Wang, L., Quan, X., and Wang, W.: Morphology, composition and mixing state of individual carbonaceous aerosol in urban Shanghai, Atmos. Chem. Phys., 12, 693–707, doi:10.5194/acp-12-693-2012, 2012.
Gross, D. S., Galli, M. E., Silva, P. J., and Prather, K. A.: Relative sensitivity factors for alkali metal and ammonium cations in single particle aerosol time-of-flight mass spectra, Anal. Chem., 72, 416–422, 2000.
Gross, D. S., Galli, M. E., Kalberer, M., Prevot, A. S. H., Dommen, J., Alfarra, M. R., Duplissy, J., Gaeggeler, K., Gascho, A., Metzger, A., and Baltensperger, U.: Real-time measurement of oligomeric species in secondary organic aerosol with the aerosol time-of-flight mass spectrometer, Anal. Chem., 78, 2130–2137, doi:10.1021/ac060138l, 2006.
Healy, R. M., Sciare, J., Poulain, L., Kamili, K., Merkel, M., Müller, T., Wiedensohler, A., Eckhardt, S., Stohl, A., Sarda-Estève, R., McGillicuddy, E., O'Connor, I. P., Sodeau, J. R., and Wenger, J. C.: Sources and mixing state of size-resolved elemental carbon particles in a

ACPD
12, 32707–32739, 2012

European megacity: Paris, Atmos. Chem. Phys., 12, 1681–1700, doi:10.5194/acp-12-1681-2012, 2012.
Hu, M., Wu, Z., Slanina, J., Lin, P., Liu, S., and Zeng, L.: Acidic gases, ammonia and water-soluble ions in $PM_{2.5}$ at a coastal site in the Pearl River Delta, China, Atmos. Environ., 42, 6310–6320, 2008.
Huang, X. F., Yu, J. Z., He, L. Y., and Hu, M.: Size distribution characteristics of elemental carbon emitted from Chinese vehicles: Results of a tunnel study and atmospheric implications, Environ. Sci. Technol., 40, 5355–5360, 2006.
Huang, X. F., Sun, T. L., Zeng, L. W., Yu, G. H., and Luan, S. J.: Black carbon aerosol characterization in a coastal city in South China using a single particle soot photometer, Atmos. Environ., 51, 21–28, doi:10.1016/j.atmosenv.2012.01.056, 2012.
Jacobson, M. C., Hansson, H. C., Noone, K. J., and Charlson, R. J.: Organic atmospheric aerosols: review and state of the science, Rev. Geophys., 38, 267–294, 2000.
Jacobson, M. Z.: Strong radiative heating due to the mixing state of black carbon in atmospheric aerosols, Nature, 409, 695–697, 2001.
Jacobson, M. Z.: Effects of externally-through-internally-mixed soot inclusions within clouds and precipitation on global climate, J. Phys. Chem. A, 110, 6860–6873, doi:10.1021/Jp056391r, 2006.
Jang, M., Czoschke, N. M., Lee, S., and Kamens, R. M.: Heterogeneous atmospheric aerosol production by acid-catalyzed particle-phase reactions, Science, 298, 814–817, 2002.
Johnson, K. S., Zuberi, B., Molina, L. T., Molina, M. J., Iedema, M. J., Cowin, J. P., Gaspar, D. J., Wang, C., and Laskin, A.: Processing of soot in an urban environment: case study from the Mexico City Metropolitan Area, Atmos. Chem. Phys., 5, 3033–3043, doi:10.5194/acp-5-3033-2005, 2005.
Kanakidou, M., Seinfeld, J. H., Pandis, S. N., Barnes, I., Dentener, F. J., Facchini, M. C., Van Dingenen, R., Ervens, B., Nenes, A., Nielsen, C. J., Swietlicki, E., Putaud, J. P., Balkanski, Y., Fuzzi, S., Horth, J., Moortgat, G. K., Winterhalter, R., Myhre, C. E. L., Tsigaridis, K., Vignati, E., Stephanou, E. G., and Wilson, J.: Organic aerosol and global climate modelling: a review, Atmos. Chem. Phys., 5, 1053–1123, doi:10.5194/acp-5-1053-2005, 2005.
Khalizov, A. F., Zhang, R., Zhang, D., Xue, H., Pagels, J., and McMurry, P. H.: Formation of highly hygroscopic soot aerosols upon internal mixing with sulfuric acid vapor, J. Geophys. Res., 114, D05208, doi:10.1029/2008jd010595, 2009.

ACPD
12, 32707–32739, 2012

Kirchstetter, T., Novakov, T., and Hobbs, P.: Evidence that the spectral dependence of light absorption by aerosols is affected by organic carbon, J. Geophys. Res., 109, D21208, doi:10.1029/2004jd004999, 2004.
Li, L., Huang, Z. X., Dong, J. G., Li, M., Gao, W., Nian, H. Q., Fu, Z., Zhang, G. H., Bi, X. H., Cheng, P., and Zhou, Z.: Real time bipolar time-of-flight mass spectrometer for analyzing single aerosol particles, Int. J. Mass. Spectrom., 303, 118–124, doi:10.1016/j.ijms.2011.01.017, 2011.
Li, W. J., Shao, L. Y., and Buseck, P. R.: Haze types in Beijing and the influence of agricultural biomass burning, Atmos. Chem. Phys., 10, 8119–8130, doi:10.5194/acp-10-8119-2010, 2010.
Lim, Y. B., Tan, Y., Perri, M. J., Seitzinger, S. P., and Turpin, B. J.: Aqueous chemistry and its role in secondary organic aerosol (SOA) formation, Atmos. Chem. Phys., 10, 10521–10539, doi:10.5194/acp-10-10521-2010, 2010.
Liu, D. Y., Wenzel, R. J., and Prather, K. A.: Aerosol time-of-flight mass spectrometry during the Atlanta Supersite Experiment: 1. Measurements, J. Geophys. Res.-Atmos., 108, 8426, doi:10.1029/2001JD001562, 2003.
Moffet, R. C. and Prather, K. A.: In-situ measurements of the mixing state and optical properties of soot with implications for radiative forcing estimates, P. Natl. Acad. Sci. USA, 106, 11872–11877, doi:10.1073/pnas.0900040106, 2009.
Moffet, R. C., de Foy, B., Molina, L. T., Molina, M. J., and Prather, K. A.: Measurement of ambient aerosols in northern Mexico City by single particle mass spectrometry, Atmos. Chem. Phys., 8, 4499–4516, doi:10.5194/acp-8-4499-2008, 2008.
Moldanová, J., Fridell, E., Popovicheva, O., Demirdjian, B., Tishkova, V., Faccinetto, A., and Focsa, C.: Characterisation of particulate matter and gaseous emissions from a large ship diesel engine, Atmos. Environ., 43, 2632–2641, doi:10.1016/j.atmosenv.2009.02.008, 2009.
Munger, J. W., Tiller, C., and Hoffmann, M. R.: Identification of Hydroxymethanesulfonate in Fog Water, Science, 231, 247–249, 1986.
Pöschl, U.: Atmospheric aerosols: composition, transformation, climate and health effects, Angew. Chem. Int. Ed., 44, 7520–7540, 2005.
Pathak, R. K., Wang, T., and Wu, W. S.: Nighttime enhancement of $PM_{2.5}$ nitrate in ammonia-poor atmospheric conditions in Beijing and Shanghai: Plausible contributions of heterogeneous hydrolysis of N_2O_5 and HNO_3 partitioning, Atmos. Environ., 45, 1183–1191, doi:10.1016/j.atmosenv.2010.09.003, 2011.

ACPD
12, 32707–32739, 2012

Pratt, K. A., Murphy, S. M., Subramanian, R., DeMott, P. J., Kok, G. L., Campos, T., Rogers, D. C., Prenni, A. J., Heymsfield, A. J., Seinfeld, J. H., and Prather, K. A.: Flight-based chemical characterization of biomass burning aerosols within two prescribed burn smoke plumes, Atmos. Chem. Phys., 11, 12549–12565, doi:10.5194/acp-11-12549-2011, 2011.

Ramanathan, V. and Carmichael, G.: Global and regional climate changes due to black carbon, Nat. Geosci., 1, 221–227, 2008.

Rehbein, P. J. G., Jeong, C. H., McGuire, M. L., Yao, X. H., Corbin, J. C., and Evans, G. J.: Cloud and Fog Processing Enhanced Gas-to-Particle Partitioning of Trimethylamine, Environ. Sci. Technol., 45, 4346–4352, doi:10.1021/es1042113, 2011.

Reinard, M. S., Adou, K., Martini, J. M., and Johnston, M. V.: Source characterization and identification by real-time single particle mass spectrometry, Atmos. Environ., 41, 9397–9409, doi:10.1016/j.atmosenv.2007.09.001, 2007.

Riipinen, I., Pierce, J. R., Yli-Juuti, T., Nieminen, T., Häkkinen, S., Ehn, M., Junninen, H., Lehtipalo, K., Petäjä, T., Slowik, J., Chang, R., Shantz, N. C., Abbatt, J., Leaitch, W. R., Kerminen, V.-M., Worsnop, D. R., Pandis, S. N., Donahue, N. M., and Kulmala, M.: Organic condensation: a vital link connecting aerosol formation to cloud condensation nuclei (CCN) concentrations, Atmos. Chem. Phys., 11, 3865–3878, doi:10.5194/acp-11-3865-2011, 2011.

Safai, P. D., Kewat, S., Pandithurai, G., Praveen, P. S., Ali, K., Tiwari, S., Rao, P. S. P., Budhawant, K. B., Saha, S. K., and Devara, P. C. S.: Aerosol characteristics during winter fog at Agra, North India, J. Atmos. Chem., 61, 101–118, 2008.

Shields, L. G., Suess, D. T., and Prather, K. A.: Determination of single particle mass spectral signatures from heavy-duty diesel vehicle emissions for $PM_{2.5}$ source apportionment, Atmos. Environ., 41, 3841–3852, 2007.

Silva, P. J. and Prather, K. A.: Interpretation of mass spectra from organic compounds in aerosol time-of-flight mass spectrometry, Anal. Chem., 72, 3553–3562, 2000.

Sodeman, D. A., Toner, S. M., and Prather, K. A.: Determination of single particle mass spectral signatures from light-duty vehicle emissions, Environ. Sci. Technol., 39, 4569–4580, 2005.

Song, X. H., Hopke, P. K., Fergenson, D. P., and Prather, K. A.: Classification of single particles analyzed by ATOFMS using an artificial neural network, ART-2A, Anal. Chem., 71, 860–865, 1999.

ACPD

12, 32707–32739, 2012

Spencer, M. T., Shields, L. G., Sodeman, D. A., Toner, S. M., and Prather, K. A.: Comparison of oil and fuel particle chemical signatures with particle emissions from heavy and light duty vehicles, Atmos. Environ., 40, 5224–5235, 2006.

Sun, J. and Ariya, P.: Atmospheric organic and bio-aerosols as cloud condensation nuclei (CCN): a review, Atmos. Environ., 40, 795–820, 2006.

Surratt, J. D., Lewandowski, M., Offenberg, J. H., Jaoui, M., Kleindienst, T. E., Edney, E. O., and Seinfeld, J. H.: Effect of acidity on secondary organic aerosol formation from isoprene, Environ. Sci. Technol., 41, 5363–5369, doi:10.1021/es0704176, 2007.

Svenningsson, B., Rissler, J., Swietlicki, E., Mircea, M., Bilde, M., Facchini, M. C., Decesari, S., Fuzzi, S., Zhou, J., Mønster, J., and Rosenørn, T.: Hygroscopic growth and critical supersaturations for mixed aerosol particles of inorganic and organic compounds of atmospheric relevance, Atmos. Chem. Phys., 6, 1937–1952, doi:10.5194/acp-6-1937-2006, 2006.

Tan, J. H., Duan, J. C., Chen, D. H., Wang, X. H., Guo, S. J., Bi, X. H., Sheng, G. Y., He, K. B., and Fu, J. M.: Chemical characteristics of haze during summer and winter in Guangzhou, Atmos. Res., 94, 238–245, 2009.

Tolocka, M. P., Lake, D. A., Johnston, M. V., and Wexler, A. S.: Number concentrations of fine and ultrafine particles containing metals, Atmos. Environ., 38, 3263–3273, doi:10.1016/j.atmosenv.2004.03.010, 2004.

Toner, S. M., Sodeman, D. A., and Prather, K. A.: Single particle characterization of ultrafine and accumulation mode particles from heavy duty diesel vehicles using aerosol time-of-flight mass spectrometry, Environ. Sci. Technol., 40, 3912–3921, doi:10.1021/es051455x, 2006.

Toner, S. M., Shields, L. G., Sodeman, D. A., and Prather, K. A.: Using mass spectral source signatures to apportion exhaust particles from gasoline and diesel powered vehicles in a freeway study using UF-ATOFMS, Atmos. Environ., 42, 568–581, 2008.

Turpin, B. J. and Huntzicker, J. J.: Identification of secondary organic aerosol episodes and quantitation of primary and secondary organic aerosol concentrations during SCAQS, Atmos. Environ., 29, 3527–3544, 1995.

Wang, W., Ren, L., Zhang, Y., Chen, J., Liu, H., Bao, L., Fan, S., and Tang, D.: Aircraft measurements of gaseous pollutants and particulate matter over Pearl River Delta in China, Atmos. Environ., 42, 6187–6202, 2008.

Whiteaker, J. R. and Prather, K. A.: Hydroxymethanesulfonate as a tracer for fog processing of individual aerosol particles, Atmos. Environ., 37, 1033–1043, 2003.

ACPD

12, 32707–32739, 2012

Xiao, R., Takegawa, N., Kondo, Y., Miyazaki, Y., Miyakawa, T., Hu, M., Shao, M., Zeng, L. M., Hofzumahaus, A., Holland, F., Lu, K., Sugimoto, N., Zhao, Y., and Zhang, Y. H.: Formation of submicron sulfate and organic aerosols in the outflow from the urban region of the Pearl River Delta in China, Atmos. Environ., 43, 3754–3763, 2009.

Yu, H., Wu, C., Wu, D., and Yu, J. Z.: Size distributions of elemental carbon and its contribution to light extinction in urban and rural locations in the pearl river delta region, China, Atmos. Chem. Phys., 10, 5107–5119, doi:10.5194/acp-10-5107-2010, 2010.

Zaveri, R. A., Berkowitz, C. M., Brechtel, F. J., Gilles, M. K., Hubbe, J. M., Jayne, J. T., Kleinman, L. I., Laskin, A., Madronich, S., Onasch, T. B., Pekour, M. S., Springston, S. R., Thornton, J. A., Tivanski, A. V., and Worsnop, D. R.: Nighttime chemical evolution of aerosol and trace gases in a power plant plume: implications for secondary organic nitrate and organosulfate aerosol formation, NO_3 radical chemistry, and N_2O_5 heterogeneous hydrolysis, J. Geophys. Res.-Atmos., 115, D12304, doi:10.1029/2009jd013250, 2010.

Zhang, G. H., Bi, X. H., Chan, L. Y., Li, L., Wang, X. M., Feng, J. L., Sheng, G. Y., Fu, J. M., Li, M., and Zhou, Z.: Enhanced trimethylamine-containing particles during fog events detected by single particle aerosol mass spectrometry in urban Guangzhou, China, Atmos. Environ., 55, 121–126, doi:10.1016/j.atmosenv.2012.03.038, 2012.

Zhang, Z., Engling, G., Lin, C. Y., Chou, C. C. K., Lung, S. C. C., Chang, S. Y., Fan, S. J., Chan, C. Y., and Zhang, Y. H.: Chemical speciation, transport and contribution of biomass burning smoke to ambient aerosol in Guangzhou, a mega city of China, Atmos. Environ., 44, 3187–3195, doi:10.1016/j.atmosenv.2010.05.024, 2010.

Zuberi, B., Johnson, K., Aleks, G., Molina, L., Molina, M., and Laskin, A.: Hydrophilic properties of aged soot, Geophys. Res. Lett., 32, L01807, doi:10.1029/2004GL021496, 2005.

ACPD
12, 32707–32739, 2012

Table 1. Summary of number count and fraction of single particle classes during spring and fall sampling periods.

Single particle classes	Number count		Number fraction[1]		Scaled number fraction
	Spring	Fall	Spring	Fall	Spring
Biomass	164 590	436 921	23.6 %	61.0 %	13.7 %
OC	69 551	82 508	10.0 %	11.5 %	10.7 %
ECOC	181 885	21 842	26.1 %	3.0 %	4.8 %
EC-fresh	32 279	6961	4.6 %	1.0 %	13.6 %
EC-Sulfate	60 230	81 226	8.6 %	11.4 %	41.5 %
V-ECOC	12 905	885	1.9 %	0.1 %	0.8 %
Amine	23 671	–[2]	3.4 %	–	0.6 %
Others	151 354	85 822	21.8 %	12.0 %	14.3 %
Sea salt	30 213	8812	4.3 %	1.2 %	
Dust-Ca	26 298	–	3.8 %	–	
Dust-Fe	20 551	2273	3.0 %	0.3 %	
Phosphate	1716	3524	0.3 %	0.5 %	
Silicate	–	2349	–	0.3 %	

[1] Number fraction was calculated through dividing the number count of single particle classes by the total particle count.
[2] The particle class was not identified during this period.

ACPD
12, 32707–32739, 2012

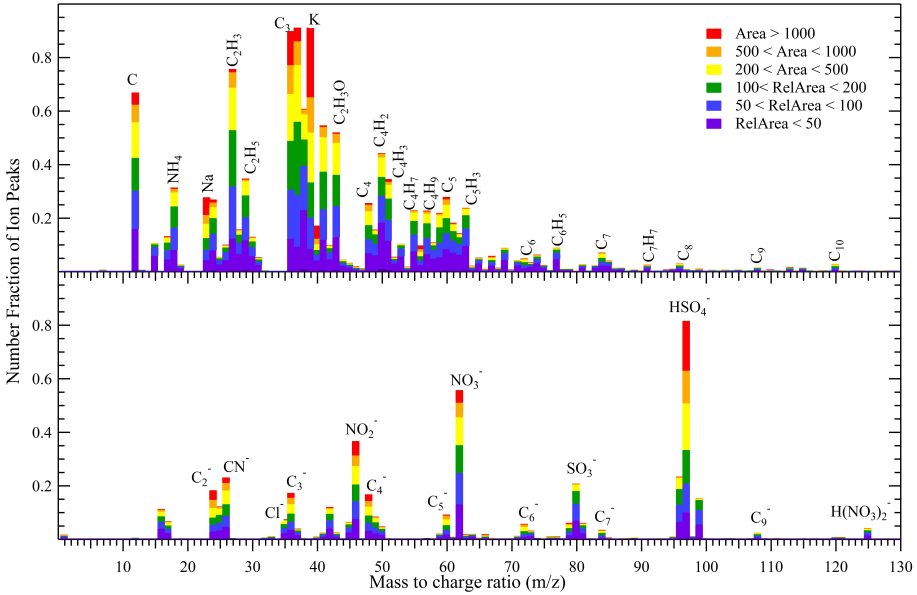

Fig. 1. Average digitized positive (upper) and negative (bottom) ions mass spectrum of carbon-containing particles analyzed over the spring period, while that for the fall period was generally similar.

ACPD
12, 32707–32739, 2012

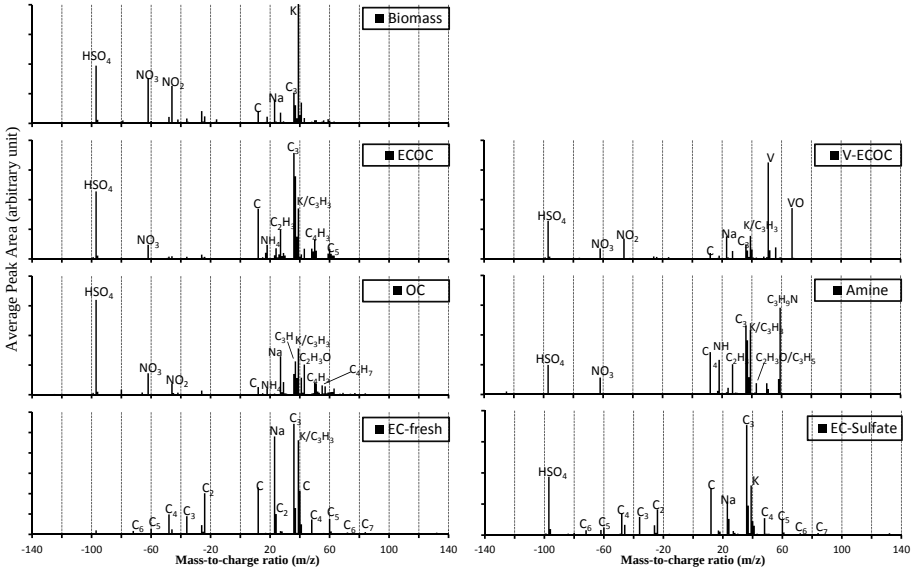

Fig. 2. Averaged positive and negative mass spectra for the 7 single particle classes (Biomass, ECOC, OC, EC-fresh, EC-Sulfate, V-ECOC, and Amine) observed during the whole sampling period in spring.

ACPD
12, 32707–32739, 2012

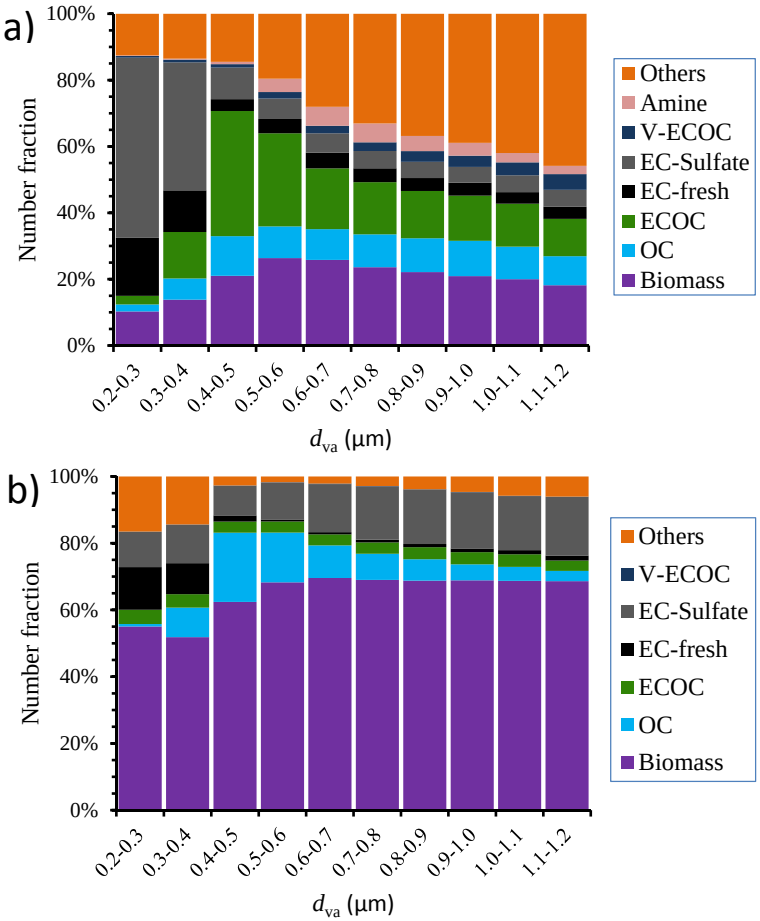

Fig. 3. Size-resolved number fractions of single particle classes for spring **(a)** and fall **(b)** period.

ACPD
12, 32707–32739, 2012

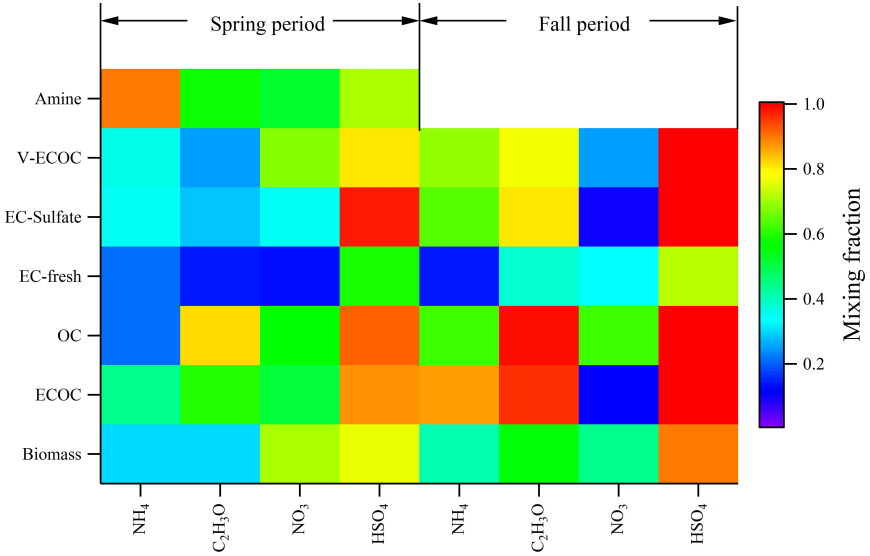

Fig. 4. Mixing state of secondary markers on the various carbon-containing particle classes. The color dots represent the number fraction of particle classes (y-axis) that contained the secondary makers (x-axis).

ACPD
12, 32707–32739, 2012

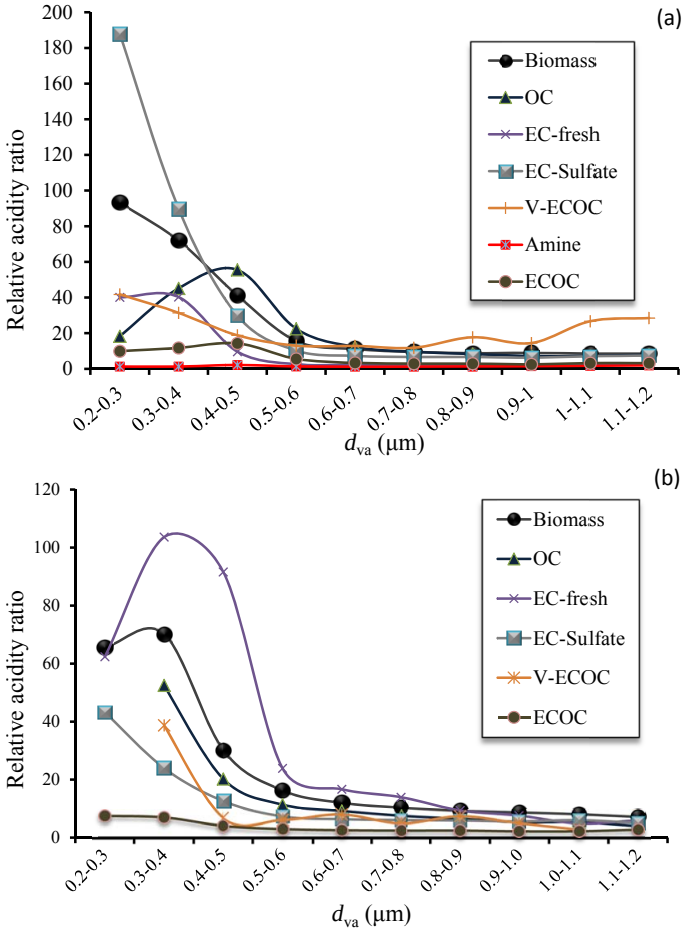

Fig. 5. Relative acidity ratio of each single particle classes as a function of d_{va} for spring **(a)** and fall periods **(b)**, respectively.

ACPD
12, 32707–32739, 2012

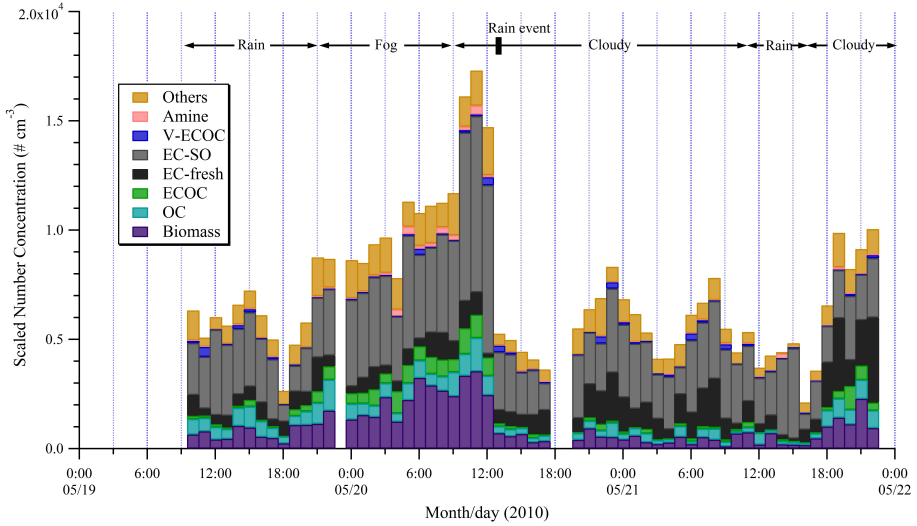

Fig. 6. Temporal profile of the scaled number concentration for each single particle class during 19–22 May 2010.

ACPD
12, 32707–32739, 2012

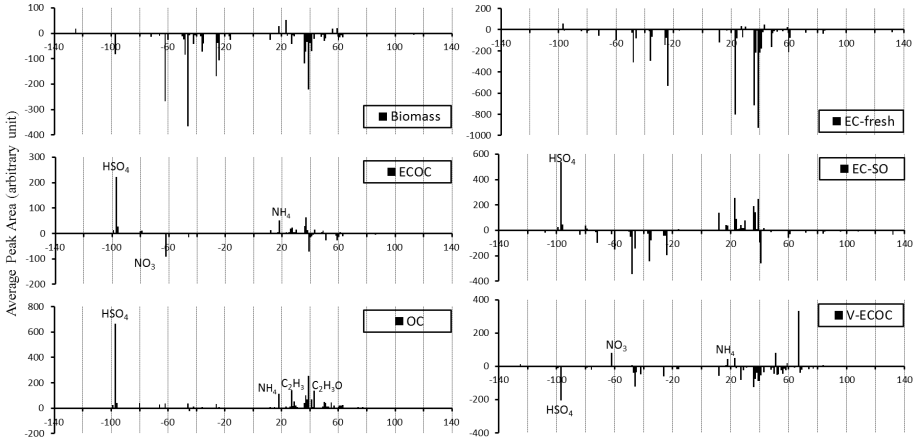

Fig. 7. Difference between mass spectra for single particle classes before and after foggy episode, calculated by subtracting the average peak areas of each single particle type before the foggy episode from those after the episode.

ACPD
12, 32707–32739, 2012

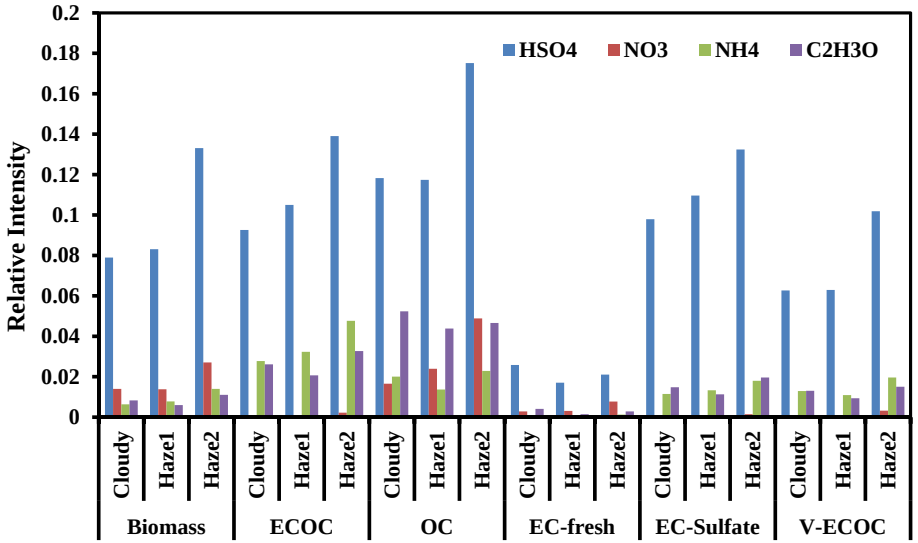

Fig. 8. Relative intensities of secondary species on each carbon-containing particle class during cloudy and hazy periods in fall.

ACPD
12, 32707–32739, 2012